



Biochemical characterization and novel inhibitor identification of *Mycobacterium tuberculosis* Endonuclease VIII 2 (Rv3297)



Kiran Lata, Mohammad Afsar, Ravishankar Ramachandran*

Molecular and Structural Biology Division, CSIR-Central Drug Research Institute, Sector 10, Jankipuram Extension, Lucknow, Uttar Pradesh 226031, India

ARTICLE INFO

Chemical compounds:

NSC31867 (Pubchem CID: 233380)

NSC345647 (Pubchem CID: 53277)

NSC250430 (Pubchem CID: 317611)

Keywords:

ROS

BER

Glycosylases

Endonuclease VIII 2

BER inhibitors

ABSTRACT

Nei2 (Rv3297) is a DNA Base Excision Repair (BER) glycosylase that is essential for survival of *Mycobacterium tuberculosis* in primates. We show that MtbNei2 is a bifunctional glycosylase that specifically acts on oxidized pyrimidine-containing single-stranded, double-stranded, 5'/3' fork and bubble DNA substrates. MtbNei2 possesses Uracil DNA glycosylase activity unlike *E. coli* Nei. Mutational studies demonstrate that Pro2 and Glu3 located in the active site are essential for glycosylase activity of MtbNei2. Mutational analysis demonstrated that an unstructured C-terminal zinc finger domain that was important for activity in *E. coli* Nei and Fpg, was not required for the glycosylase activity of MtbNei2. Lastly, we screened the NCI natural product compound database and identified three natural product inhibitors with IC50 values ranging between 41.8 μ M–92.7 μ M against MtbNei2 in in vitro inhibition assays. Surface Plasmon Resonance (SPR) experiments showed that the binding affinity of the best inhibitor, NSC31867, was 74 nM. The present results set the stage for exploiting this important target in developing new therapeutic strategies that target Mycobacterial BER.

1. Introduction

Tuberculosis (TB) causes 1.8 million deaths worldwide each year. Cases of drug-resistant (MDR) TB have also risen to more than half a million globally (**WHO 2016 Global Tuberculosis report**). *Mycobacterium tuberculosis* is an intracellular pathogen that dwells in alveolar macrophages and encounters a diverse range of oxidative stress conditions viz. reactive oxygen and nitrogen intermediates. These free radicals cause DNA base damages. Oxidative DNA damage is mainly repaired by the premier base-excision repair (BER) pathway [1,2]. BER initiates with the recognition of the damaged base by DNA glycosylases. Monofunctional DNA glycosylases cleave the N-glycosyl bond between the damaged base and the sugar creating an abasic (AP) site. However, bifunctional DNA glycosylases also possess an associated AP-lyase activity that cleaves the phosphodiester bond at the AP site by a β - or β - δ elimination mechanism generating either an α , β -unsaturated aldehyde (β -elimination) or a phosphate (β , δ -elimination) group [3].

Based on structural and sequence homology, DNA glycosylases are generally classified into two families viz. the Fpg/Nei superfamily and the Nth superfamily [4,5]. The Fpg/Nei superfamily includes formamidopyrimidine DNA glycosylase or Fpg, also known as MutM,

which recognizes both 8-oxoguanine and formamidopyrimidines while Endonuclease VIII (Nei) specifically recognizes oxidized pyrimidines and uracils [6,7]. Fpg is a structural homologue of Nei while Nth is a functional homologue.

Nei proteins consist typically of two domains which are connected by a flexible hinge region. The N-terminal region contains a β -sandwich flanked by α -helices. The C-terminal domain consists of α -helices, two of which form a conserved H2TH motif, and a Zn-finger motif formed by two antiparallel β -strands. These motifs are found in both Fpg and Nei subfamilies and additionally the zinc finger and H2TH motifs in Fpg are required for DNA binding [7,8, and 9].

The catalytic mechanism of Nei comprises multiple steps and involves nucleophile attack at the C1' position of the target nucleotide by an N-terminal proline (Pro2) residue. Glu 3, and a lysine that aligns with position 53 in EcoNei are also important for the activity [10].

Structures of EcoNei with lesion containing duplex DNA are available and have shown that DNA binds to a positively charged groove of the enzyme and also the damaged base is extruded through the major groove. A DNA kink of about 45° occurs at the lesion point upon enzyme binding to enable catalysis. The latter EcoNei–DNA complex is stabilized, amongst other things, by interactions involving Gln69, Leu70 and

Abbreviations: TB, tuberculosis; ROS, reactive oxygen species; *Mtb*, *Mycobacterium tuberculosis*; BER, base excision repair; MtbNei2, *M. tuberculosis* Endonuclease VIII 2; MtbNei2 Δ ZNF, *M. tuberculosis* zinc finger domain deleted mutant; MDR, multidrug resistance; AP, apurinic/aprimidinic; EcoNei, *E. coli* Endonuclease VIII; EcoFpg, *E. coli* Formamidopyrimidine glycosylase; SEC, size exclusion chromatography

* Corresponding author.

E-mail address: r_ravishankar@cdri.res.in (R. Ramachandran).

<http://dx.doi.org/10.1016/j.bbrep.2017.07.010>

Received 29 March 2017; Received in revised form 10 July 2017; Accepted 29 July 2017

Available online 31 July 2017

2405-5808/ © 2017 The Authors. Published by Elsevier B.V. This is an open access article under the CC BY-NC-ND license (<http://creativecommons.org/licenses/by-nc-nd/4.0/>).

Tyr71 [10].

Nei occurs in actinobacteria and some γ -proteobacteria, and it has been suggested that it is of relatively recent origin [5,6]. The *Mtb* genome has two paralogs viz. MtbNei1 (Rv2464c) and MtbNei2 (Rv3297). Biochemical characterization of MtbNei1 protein has been reported by two groups. Sidorenko et. al. 2008 showed MtbNei1 (named as MtuNei2 in their study) to remove oxidized pyrimidines and possesses AP site cleavage activity [11]. Guo et. al. reported MtbNei1 to be active on uracil containing DNA substrates [7]. Though, MtbNei2 has been shown to complement the spontaneous mutation frequencies in *E. coli fpg mutY nei* triple and *E. coli nei nth* double mutants, its biochemical characterization has not been reported yet [7]. Although, *nei2*(Rv3297) is not essential for in vitro survival of the pathogen, it is required for successful infection and growth of *Mtb* in primate hosts [12].

In the present study, we cloned and purified MtbNei2 (Rv3297). We biochemically characterized MtbNei2 and carried out mutational analysis to identify catalytically important residues. Interestingly, we identified that a C-terminal Zinc-finger domain that was reported to be important for activity in the *E. coli* Fpg and Nei proteins, is dispensable for glycosylase activity of MtbNei2. Finally, we identified 3 natural product inhibitors of the enzyme following a rational screening experiment. The best of these inhibitors binds to MtbNei2 with a Kd of 74 nM.

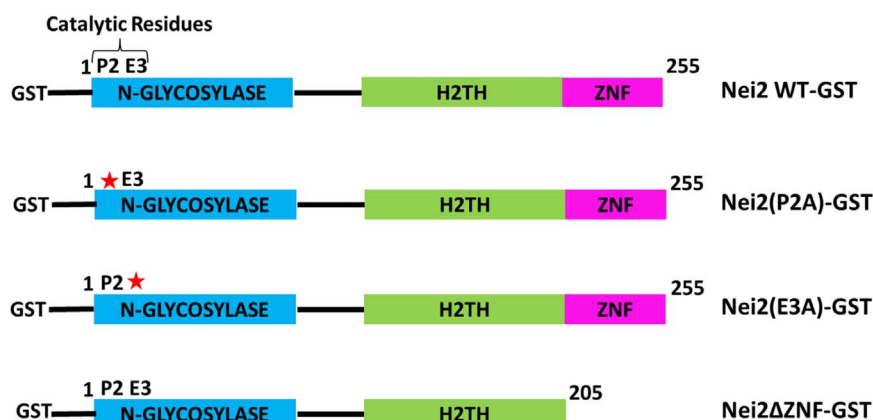
2. Materials and methods

2.1. Oligonucleotide substrates and proteins

A 51-mer oligonucleotide containing Uracil at position 26 from the 5'-end was purchased from *Integrated DNA Technology*, USA (IDT). The sequences of complementary oligonucleotides had Guanine opposite the lesion for generating duplex or contained non complementary sequences for producing bubble and fork structures as shown in [Table S2](#) [13]. A 51-mer oligonucleotide containing 5-OHU at position 26 from 5' end and a 35-mer oligonucleotide containing 8-oxo-G at position 14 from 5' end was purchased from Midland certified reagent company, Texas. For optimal annealing, an equimolar mixture of lesion containing and complementary strands was heated to 94 °C for 2 min in nuclease free water and then slowly cooled to room temperature. All the oligonucleotides were 6-FAM labeled at 5' end. For DNA binding studies, a 22 mer single stranded oligonucleotide substrate was synthesized from *Integrated DNA Technology*, USA. EcoFpg protein was purchased from New England Biolabs. EcoUNG protein was purchased from Fermentas ([Fig. 1](#)).

2.2. Structure modeling and alignment

A structural model of MtbNei2 was generated using *Modeller 9.10*



(http://salilab.org/modeller/download_installation.html) with the structure of the MutM (Fpg) from *Geobacillus stearothermophilus* protein (PDB: 1L1T, 29% Identity) [9] as template. The final refined model was validated using RAMPAGE [14] and more than 94% of residues were found to be in the most favorable region of the Ramachandran plot ([Fig. S4](#)). MtbNei2 model was superimposed with known Nei and Fpg crystal structures using Rapido [15] in order to locate active site, lesion recognition loop and zinc finger motifs. Visualization of structures was carried out using Chimera [16]

2.3. Cloning, expression and purification of wild-type MtbNei2 and mutants

The genomic DNA of *M. tuberculosis* H37Rv was kindly provided by Dr. Kishore K. Srivastava (Central Drug Research Institute, India). (The gene sequences were retrieved from GenBank for *M. tuberculosis* H37Rv: NP_217814 Rv3297). The MtbNei2 (Rv3297) and Zinc finger domain deletion gene sequences were PCR amplified using gene specific primers listed in [Supplementary Table S1](#) and cloned between the *Bam*HI and *Hind*III restriction sites in N-terminal GST tag containing vector pGEX-KG (GE Healthcare). The pGEX-KG-Nei2 (255 amino acids) and C-terminal zinc finger deleted mutant, pGEX-KG-Nei2ΔZNF (1–205) constructs were overexpressed in *E. coli* BL21DE3 cells using 0.5 mM IPTG (Merck). The Nei2WT-GST and Nei2ΔZNF-GST overexpressing cells were re-suspended in lysis buffer A [50 mM Tris-HCl pH-7.5, 250 mM NaCl and 1 mM PMSF] and lysed by sonication. The lysates were centrifuged at 15,000 rpm for 20 min at 4 °C and the supernatant was allowed to bind for 4 h at 4 °C with glutathione-agarose beads pre-equilibrated with buffer A. The beads were washed with 20 column volumes of buffer A. The Nei2WT-GST and Nei2ΔZNF-GST proteins eluted with buffer A containing 20 mM reduced glutathione and pH adjusted to 7.5. The eluted fractions were analyzed on 12% SDS PAGE. Purified proteins were loaded onto pre-equilibrated Superdex-200 10/300 GL column in buffer containing 50 mM Tris 7.5, 200 mM NaCl [Fig. 2](#)(A-B).

2.4. Site directed mutagenesis

Based on sequence analysis, two point mutations of residues lying in the catalytic site of MtbNei2 i.e P2A and E3A were generated using pGEX-KG-Nei2 construct as template and appropriate overlapping primers ([Table S1](#)). After initial denaturation step at 94 °C for 4 min, PCR was conducted for 25 cycles with denaturation at 94 °C for 60 s, primer annealing at 60.3 °C {for pGEX-KG-Nei2(P2A)} and 62.3 °C {for pGEX-KG-Nei2(E3A)} for 45 s and DNA synthesis at 72 °C for 60 s for each 1 kb of plasmid sequence, e. g. 6 min for a plasmid + gene sequence of 5.768 kb. The high fidelity Platinum *Pfx* DNA polymerase was used (Thermo Fisher Scientific). The products were digested overnight by *Dpn*I (Fermentas) at 37 °C to remove the template DNA and transformed into *E. coli* DH5 α . Plasmids were purified. Double digestion and

Fig. 1. Schematic diagram of constructs used in the study; Nei2WT-GST (full length, 255aa), Nei2(P2A)-GST (P2A catalytic mutant, 255aa), Nei2(E3A)-GST (E3A catalytic mutant 255aa) and Nei2ΔZNF-GST (Zinc finger domain deleted mutant, 205aa).

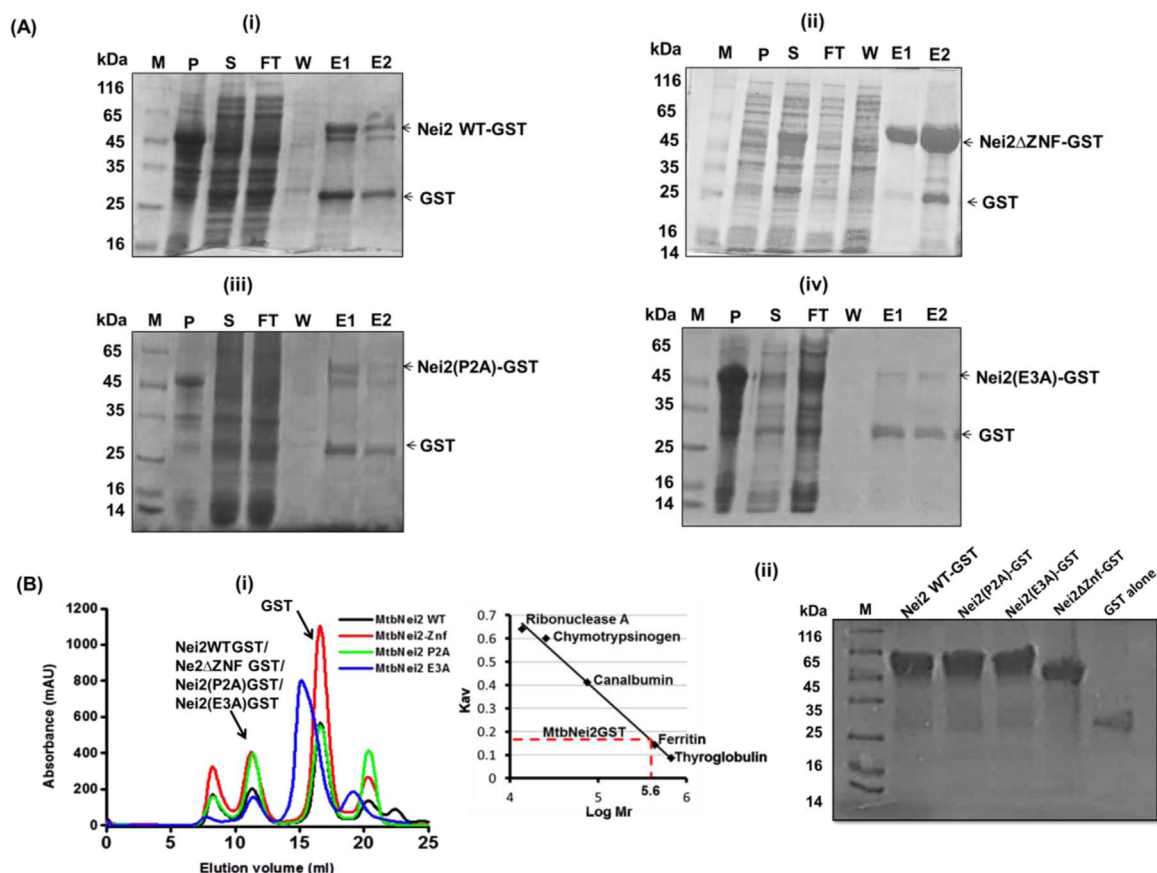


Fig. 2. A. Protein purification of Nei2 /mutants: 12% SDS PAGE of samples of GST Affinity chromatography (i) Nei2WT-GST (~ 55 kDa), (ii) Nei2 Δ ZNF-GST (~ 49 kDa), (iii) Nei2(P2A)-GST (~ 55 kDa) and (iv) Nei2(E3A)-GST (~ 55 kDa); B. Second-step purification of Nei2 /mutants using Size exclusion chromatography (SEC): Purified proteins were loaded onto a pre-equilibrated Superdex 200 10/300 GL column (G.E.Healthcare) in 50 mM Tris-HCl pH7.5, 50 mM NaCl buffer. Nei2WT-GST and all the mutants eluted as octamer at 10.9 ml elution volume. 10.9 ml peak corresponds to Nei2WT-GST (black line), Nei2 Δ ZNF-GST (red), Nei2(P2A)-GST (green) and Nei2(E3A)-GST (blue). GST alone protein eluted at 15.6 ml; Molecular weight was calculated using calibration curve of known molecular weight markers; (ii) 12% SDS PAGE of SEC eluted peak2 and 3: lane1-marker, lane2-Nei2WT-GST, lane3-Nei2(P2A)-GST, lane4-Nei2(E3A)-GST and lane5-Nei2 Δ ZNF-GST, last lane-peak3/GST alone protein. (M- marker, P-pellet, S-supernatant, FT-flow through, W-wash, E-elution). (For interpretation of the references to color in this figure legend, the reader is referred to the web version of this article).

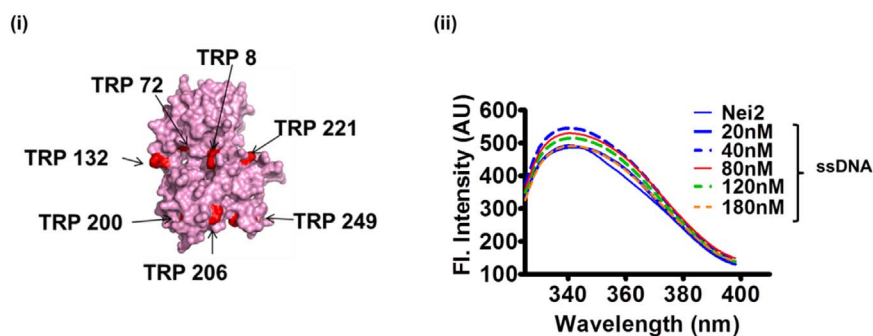


Fig. 3. DNA binding monitored using Trp fluorescence quenching. (i) Presence of Trp sites on MtbNei2; (ii) 200 nM MtbNei2 in a buffer containing 50 mM Tris-HCl pH7.5 and 50 mM NaCl was titrated with 0–180 nM ssDNA. Samples were excited at 280 nm and emission spectrum was recorded between 300 and 400 nm wavelengths.

sequencing was done (Chromous Biotech., India) to verify the mutations. *E. coli* BL21 DE3 cells were used to express and purify the verified mutant constructs pGEX-KG-Nei2(P2A) and pGEX-KG-Nei2 (E3A) using above described purification method Fig. 2(A-B).

2.5. DNA Glycosylase activity

In a 20 μ l reaction, 100 nM labeled substrate {G1(Uracil)/G2(double stranded)/G3(5'fork)/G4(3'fork), G5(bubble)/G6(5-OHU) or G7(8-oxo-G)} was incubated with increasing concentration of MtbNei2 enzyme (5 nM, 10 nM, 20 nM, 40 nM or 80 nM) in glycosylase buffer G (10 mM Tris-HCl pH8.0, 75 mM NaCl and 1 mM EDTA) supplemented with 0.1 mg/ml of BSA. The reactions were carried out at

37 $^{\circ}$ C for 30 min. All the reactions were ended with 20 μ l of formamide stop loading buffer F (98% formamide, 5 mM EDTA, 0.1% xylene cyanol and 0.1% bromophenol blue). The cleaved products and uncleaved substrates were separated on a 12% denaturing urea polyacrylamide gel and quantified using ImageQuant LAS4000 and ImageQuantTL 8.1 software (GE Healthcare) [7], (Table S2).

2.6. AP site incision activity

AP site cleavage activity was performed as described above for glycosylase assay but with an AP site containing substrate (A1) generated by annealing a 75-mer oligonucleotide containing Tetrahydrofuran, an AP site analogue to its complementary

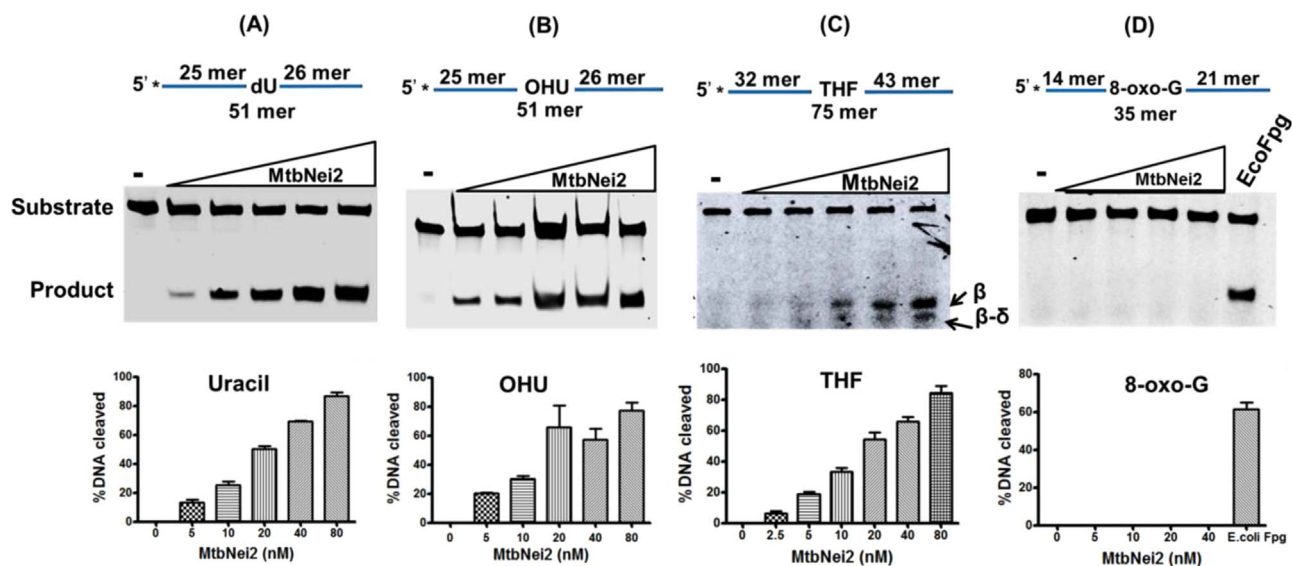


Fig. 4. Glycosylase/lyase activity of MtbNei2 on single stranded DNA containing various lesions: Labeled substrate, 100 nM, was incubated with either no enzyme (–) or increasing amounts of MtbNei2. (A), (B) and (C) Nei2WT-GST concentrations (5 nM, 10 nM, 20 nM, 40 nM, 80 nM) were tested with Uracil, 5-OHU and THF substrates; (D) Nei2WT-GST concentrations (5 nM, 10 nM, 20 nM and 40 nM) were tested with 8-oxo-G and 2 nM EcoFpg control enzyme was also included (last lane-5).

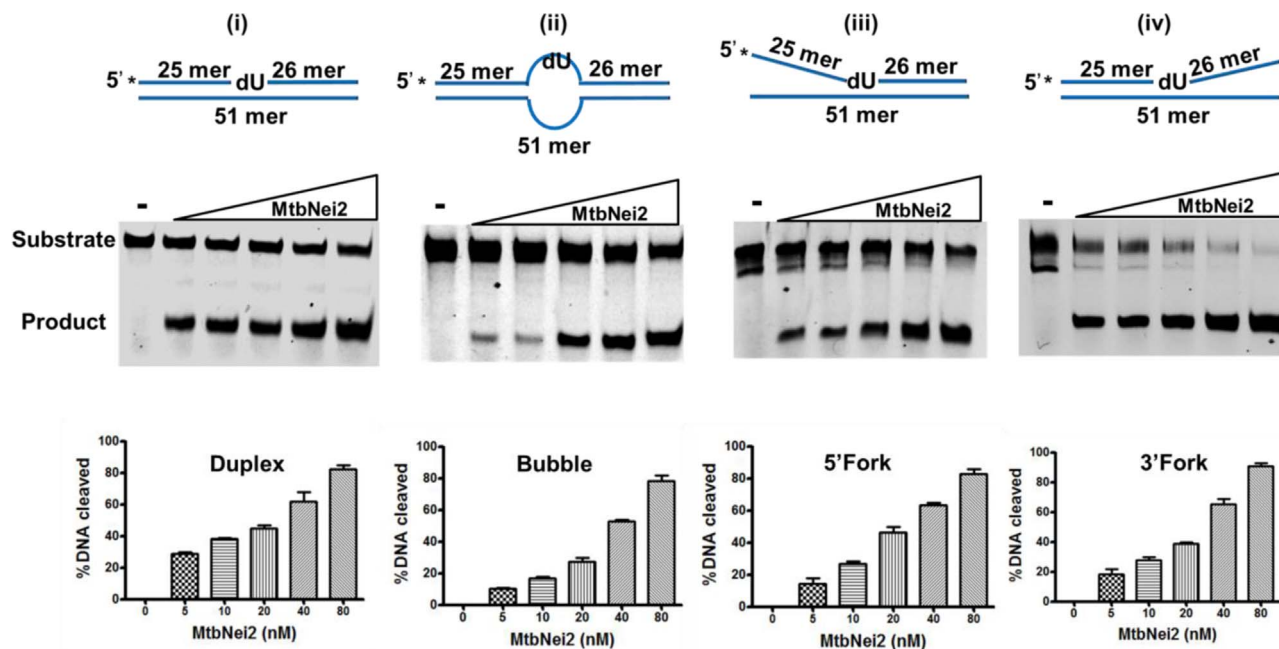


Fig. 5. Effect of DNA structures on glycosylase/lyase activity of MtbNei2 was tested by incubating 100 nM labeled uracil containing (i) duplex, (ii) bubble, (iii) 5'fork or (iv) 3'fork DNA with either no enzyme or increasing concentrations (5 nM, 10 nM, 20 nM, 40 nM, 80 nM) of MtbNei2.

oligonucleotide (Table S2).

2.7. DNA binding using tryptophan fluorescence quenching assay

MtbNei2 contains 7 tryptophan residues. Trp72 and Trp221 surround the active site pocket whose intrinsic fluorescence can be monitored for DNA binding events of MtbNei2. Variation in the intrinsic tryptophan fluorescence was checked in a solution containing 200 nM MtbNei2, 50 mM Tris-HCl pH7.5 and 50 mM NaCl. The concentration of single stranded DNA was varied (0–180 nM). Excitation wavelength used was 280 nm, while emission spectra were obtained by scanning from 300 to 400 nm using a Cary Eclipse Fluorescence Spectrophotometer (Agilent Tech. USA).

2.8. Inhibition studies

2.8.1. Virtual screening

National Cancer Institute's Natural Product database was selected for screening against MtbNei2. The reference protein coordinates for screening were obtained from the model of MtbNei2 (template PDB ID: 1L1T) [9] after being shorn off the water molecules and addition of hydrogen and required charges. The N-terminal 1-MPEGDT-5 residues were selected as the docking/screening site. All the compounds were screened in a grid surrounding the docking site using Surflex-Dock of SYBYLX2.0 [22]. A maximum of 5 poses were evaluated for each compound. Top 10 hits were selected based on the highest docking score (Chem score+ G score+ D score+ PMF score). The selected compounds were obtained from National Cancer Institute, USA and

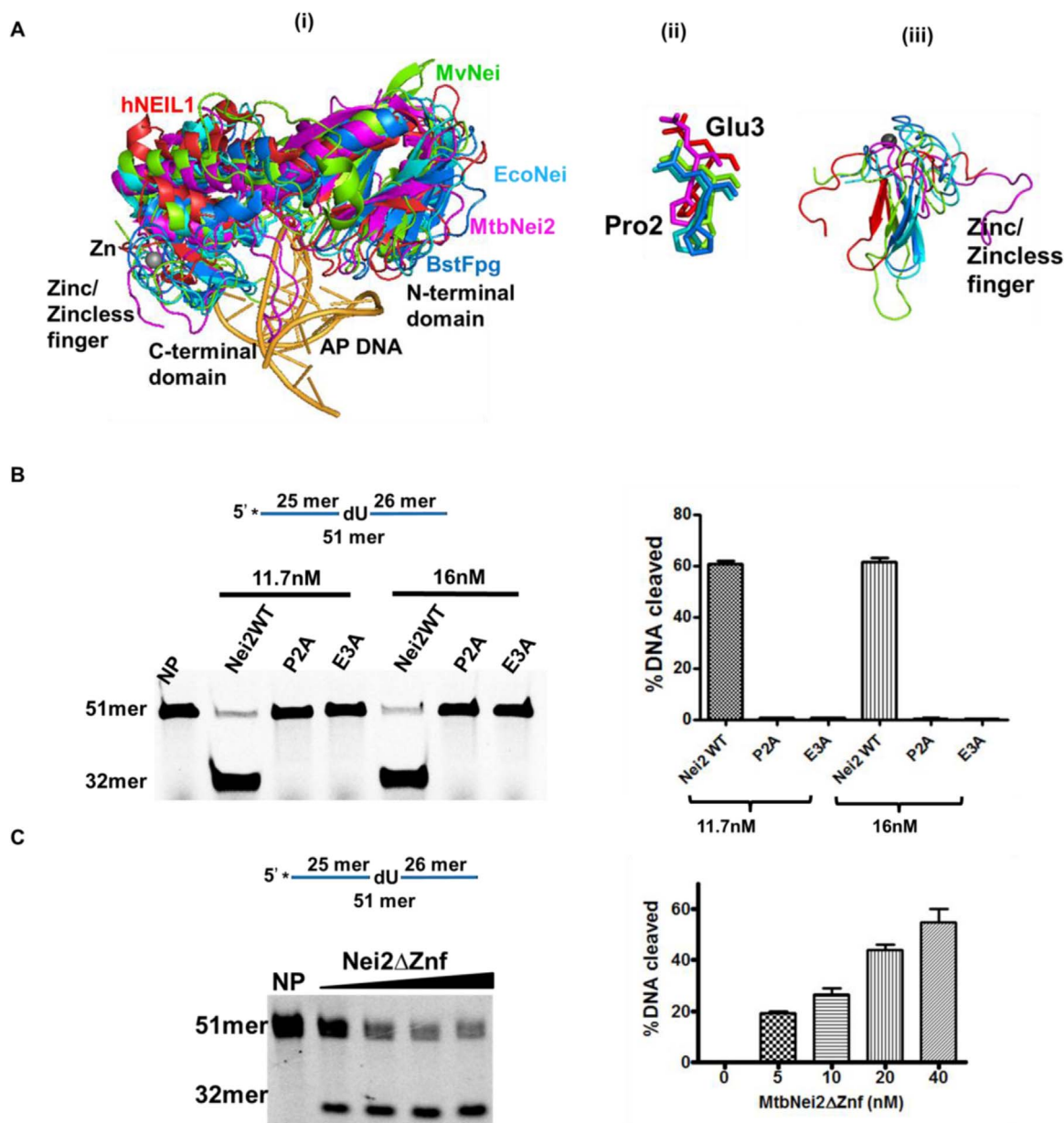


Fig. 6. Role of Pro2, Glu3 residues and Zinc finger in Nei2WT-GST. A. i) Structural alignment of MtbNei2(Rv3297) model with known Fpg/Nei family protein crystal structures (1K3W, 1L1T, 5ITT, 3A46) performed using Rapido, (ii) Conserved catalytic Pro2 and Glu3 and (iii) Zinc/zincless finger; B. Activity of catalytic/zinc finger deletion mutants: 100 nM uracil substrate was incubated with either Nei2WT-GST, Nei2(P2A)-GST or Nei2(E3A)-GST at concentrations (11.7 nM and 16 nM) or C. increasing concentrations of Nei2ΔZNF (NP-no protein, 5 nM, 10 nM, 20 nM, 40 nM). Data is indicative of two independent experiments (NP- no protein).

were further evaluated against in vitro Uracil DNA glycosylase activity of MtbNei2.

2.9. In vitro inhibition assay

In a reaction of 20 μl, 100 nM labeled single stranded DNA substrate containing Uracil/THF and 80 nM MtbNei2 was incubated with increasing concentration of inhibitors (50 μM, 100 μM, 200 μM, 400 μM and 800 μM) in buffer G. The reactions were carried out at 37 °C for 30 min. All the reactions were stopped with 20 μl of formamide stop buffer F. Cleaved and uncleaved substrates were resolved on 12% denaturing urea polyacrylamide gel and quantified using ImageQuant LAS 4000 and ImageQuantTL 8.1 software (GE Healthcare). Potency of compounds was measured by determining IC₅₀ values. IC₅₀ values were determined by plotting the % MtbNei2 activity versus inhibitor concentration using GraphPad Prism software and fitting to the equation:

$V_i/V_0 = IC_{50}/(IC_{50} + [I])$ where, V_0 and V_i are the rates of MtbNei2 glycosylase/AP lyase activity in the absence and presence of the inhibitor respectively, and $[I]$ represent the inhibitor concentration.

To gain further insights to the mode of inhibitor-protein interactions, inhibitors were docked against the MtbNei2 model using Autodock4.2 [17].

2.10. Surface plasmon resonance (SPR) binding assay

The anti-GST antibody (Santa Cruze Biotechnology) was immobilized up to 8000 response units (RU) onto a CM5 sensorchip (BIAcore3000 system, GE Healthcare) using standard amine coupling chemistry. Binding using capturing molecule methodology was employed where 7 nM MtbNei2 dialyzed in HBS buffer was injected as capturing molecule. Concentration series of NSC31867 (0, 25, 50, 100 and 200 nM) were injected in HBS (10 mM HEPES pH 7.4, 150 mM

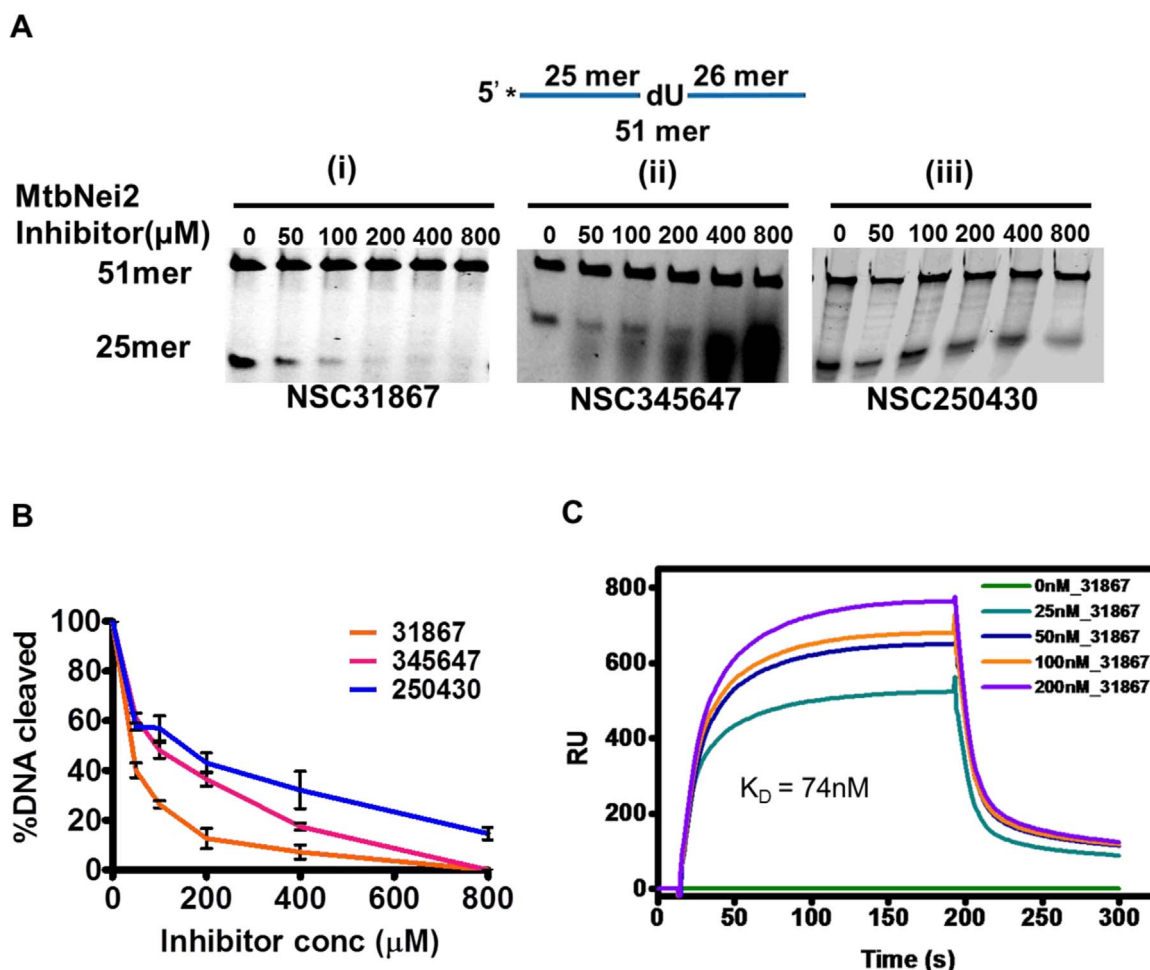
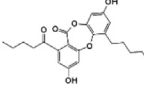
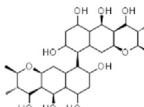
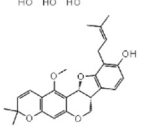


Fig. 7. A. Effect of compounds on Uracil DNA glycosylase activity of MtbNei2 (i) NSC31867, (ii) NSC345647 and (iii) NSC250430; 100 nM labeled substrate was incubated with 80 nM MtbNei2 and either no inhibitor or increasing concentrations (50 μM, 100 μM, 200 μM, 400 μM and 800 μM) of compounds; B. Inhibition curves obtained after plotting % DNA cleaved against the inhibitor concentrations; C. SPR analysis. NSC31867 (0, 25, 50, 100 and 200 nM concentrations) (solid lines; double referenced) were injected on the Nei2WT-GST captured on CM5 chip immobilized with anti-GST antibody. The sensorgrams were fitted to the 1:1 reaction model to calculate K_D as per Biacore manual.

Table 1
Inhibition studies against *in vitro* Uracil DNA glycosylase activity of MtbNei2.

S. No.	Compound Identifier	Inhibitor scaffold 2D	IC ₅₀ (μM)		Dissociation constant K _d (nM)	H-bond forming residues
			UDG activity	AP site cleavage activity		
01	NSC31867 Norlobaric acid		41.80	64.84	74nM	PRO2, ASN76, TYR166
03	NSC345647 Chaetochromin		92.71	84.68	ND	SER61, ASN76, TYR166
04	NSC250430 Gangetin		76.25	43.65	ND	ASN76, ARG77, TYR166

NaCl, 3 mM EDTA and 0.8% DMSO) at a flow rate of 30 μl/min. The binding response was measured for 150 s after the end of injection. The interactions between MtbNei2 and inhibitors were analyzed and steady-state binding was determined at each concentration. Following each injection cycle, chip surfaces were regenerated with an injection of 10 mM Glycine pH2.0. Sensorgrams were processed by BIAevaluation software (GE Healthcare) to obtain kinetic parameters of

protein–inhibitor interaction. The steady-state binding constants were determined by fitting the data to a 1:1 Langmuir isotherm as per the Biacore manual [18].

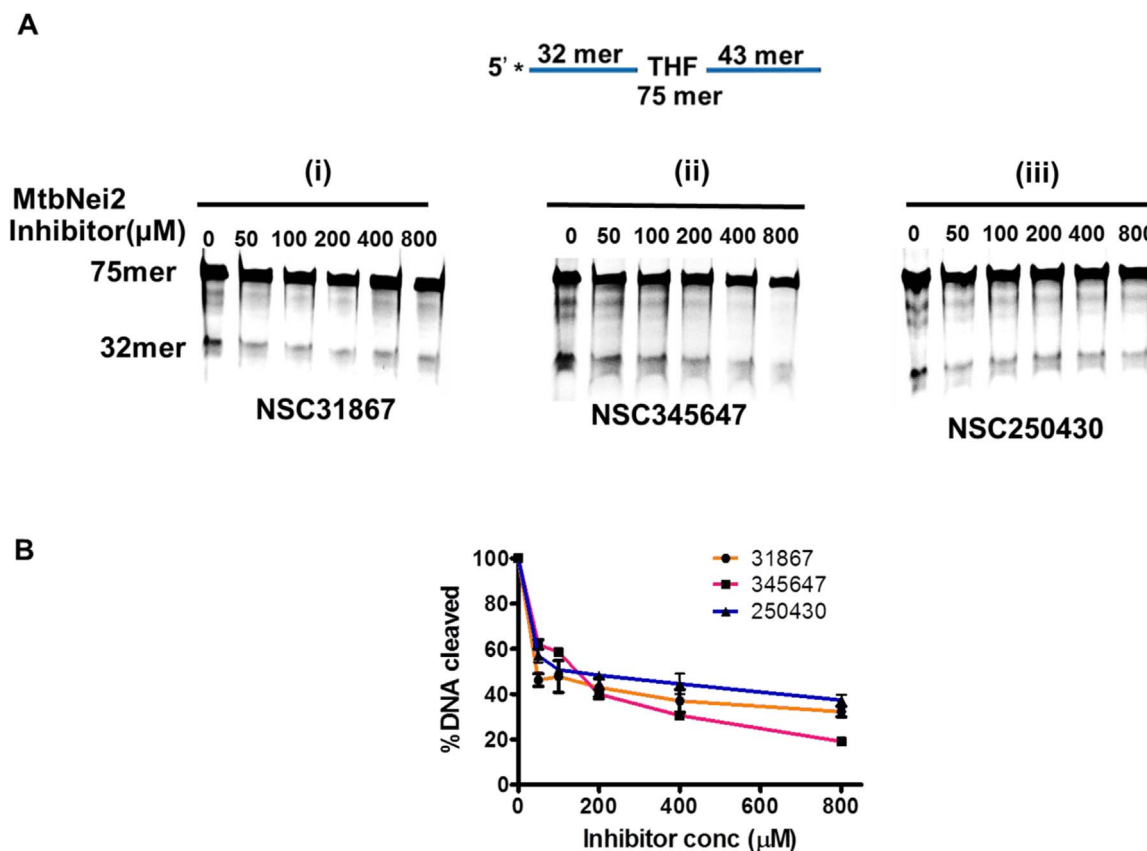


Fig. 8. Effect of compounds on AP site incision activity of MtbNei2. (i) NSC31867, (ii) NSC345647 and (iii) NSC250430; 100 nM labeled substrate was incubated with 80 nM MtbNei2 and either no inhibitor or increasing concentrations (50 μM, 100 μM, 200 μM, 400 μM and 800 μM) of compounds; B. Inhibition curves obtained after plotting % DNA cleaved against the inhibitor concentrations.

3. Results

3.1. Purification of wild-type Nei2WT-GST, Nei2ΔZNF-GST, catalytic site mutants Nei2(P2A)-GST and Nei2(E3A)-GST

MtbNei2 wild type/mutants were cloned and overexpressed (Fig. S1). Proteins Nei2WT-GST (26kDaGST + 29 kDa Nei2WT = 55 kDa), Nei2ΔZNF-GST (26 kDa GST + 23 kDa Nei2ΔZNF = 49 kDa), Nei2(P2A)-GST (26kDaGST + 29 kDa Nei2WT = 55 kDa) and Nei2(E3A)-GST (26kDaGST + 29 kDa Nei2WT = 55 kDa) were purified to homogeneity using GST affinity purification followed by SEC. SEC profile shows Nei2WT-GST wild type and mutant proteins to be octamer with elution volume of 10.9 ml (Fig. 2).

3.2. Biochemical characterization of MtbNei2

3.2.1. Undamaged DNA binding

Presence of tryptophan residues in various domains of MtbNei2 which are involved in catalysis led us to investigate the effect of DNA binding on the overall conformation of the protein by monitoring intrinsic tryptophan (Trp) fluorescence. A first increase (0–40 nM) followed by decrease in the intrinsic Trp fluorescence was observed with increasing DNA concentration from 0 to 180 nM. Change in Trp fluorescence with increase in DNA concentration suggests the protein undergoes conformational change upon binding to DNA and this probably modulates the activity (Fig. 3).

3.2.2. MtbNei2 specifically recognizes oxidized pyrimidines

We tested MtbNei2 activity on single-stranded oligodeoxynucleotide containing Uracil, 5-Hydroxy-Uracil (5-OHU) and 8-oxo-Guanine. MtbNei2 successfully recognized and cleaved the Uracil and 5-OHU

containing substrates (Fig. 4A, B). At the same time, MtbNei2 failed to cleave 8-oxo-G containing substrate whereas control enzyme EcoFpg could cleave it (Fig. 4D). The results suggest MtbNei2 specifically recognizes oxidized pyrimidines. Furthermore, MtbNei2 found to cleave the AP site substrate as well via β and β-δ eliminations as depicted by the two bands formed after the cleavage (Fig. 4C). Like other Nei and MtbNei1 proteins, MtbNei2 is a bifunctional glycosylase. In control experiments, GST alone didn't exhibit any of the above activities (Fig. S3).

3.2.3. Effect of DNA structures on MtbNei2 activity-

To investigate MtbNei2's activity on various types of DNA structures, we tested its activity on Uracil containing duplex DNA, 5'fork, 3'fork and bubble DNA substrates. MtbNei2 could recognize and remove base lesions on double stranded, 3'fork, 5'fork and bubble DNA substrates. This suggests MtbNei2 has active roles in pre-replicative and pre-transcriptional associated BER (Fig. 5).

3.3. Pro2 and Glu3 are essential active site residues of MtbNei2

The MtbNei2 mutants, Nei2(P2A)-GST and Nei2(E3A)-GST showed no activity on uracil containing substrate when compared to wild type MtbNei2 at two different enzyme concentrations (Fig. 6B). This shows that Pro2 and Glu3 are essential for MtbNei2 activity.

3.4. The C-terminal Zinc finger domain of MtbNei2 is dispensable for glycosylase activity

Activity of C-terminal Zinc finger domain deleted mutant, Nei2ΔZNF-GST was tested on Uracil containing DNA substrate. Nei2ΔZNF-GST was found to be fairly active and it successfully cleaved

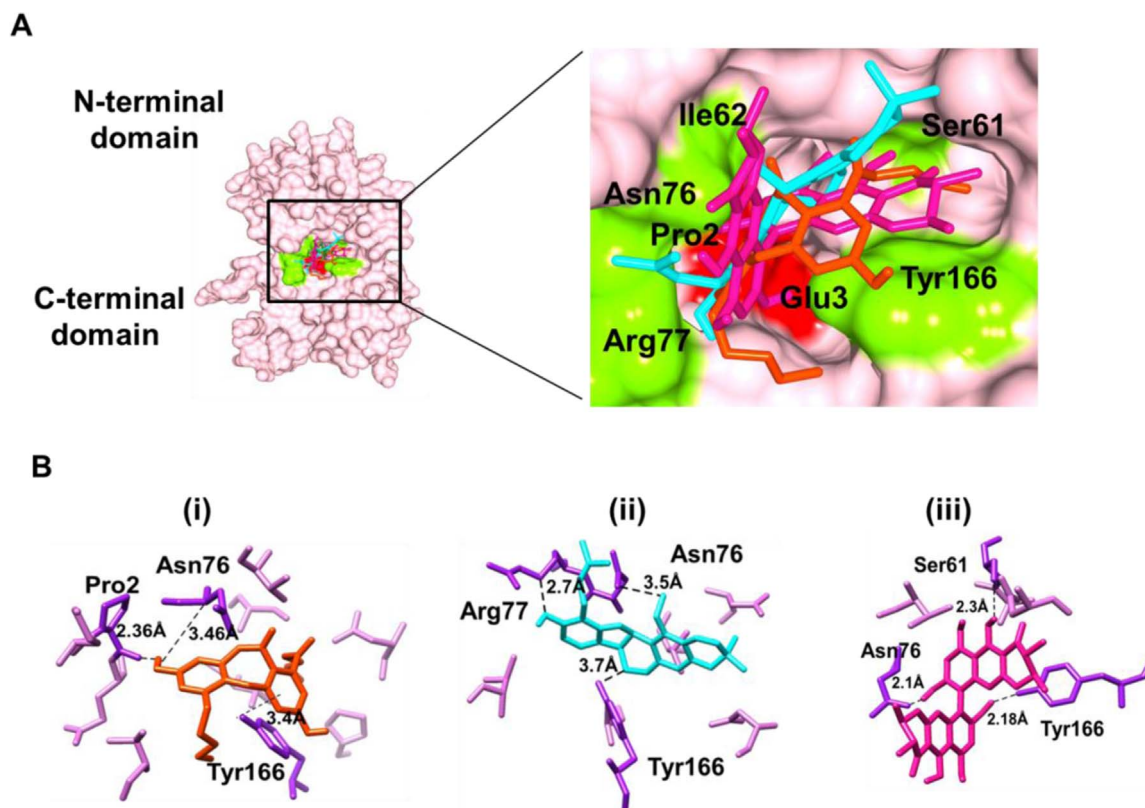


Fig. 9. Docking predicts the binding modes of inhibitors against MtbNei2. A. Inhibitors docked against inter-domain catalytic-DNA binding cleft of MtbNei2, NSC31867 (orange), NSC345647 (magenta) and NSC250430 (cyan); B. Binding modes of i) NSC31867, ii) NSC250430 and iii) NSC345647 against MtbNei2 as predicted by docking. (For interpretation of the references to color in this figure legend, the reader is referred to the web version of this article).

the uracil containing substrate (Fig. 6C). This result suggests that the Zinc-finger domain is not important for the glycosylase activity of MtbNei2 in contrast to EcoNei and Fpg where it was found to severely compromise the activity of the respective enzymes.

3.5. Identification of inhibitors against MtbNei2

Ten best scoring compounds were selected after virtual screening of the NCI natural product database against MtbNei2. These were then assayed against Uracil DNA glycosylase and AP site cleavage activities of MtbNei2. NSC31867 (Norlobaric acid), NSC345647 (Chaetochromin) and NSC250430 (Gangetin) showed good inhibition of both Uracil DNA glycosylase (Fig. 7A, B; Table 1) and AP site cleavage activity (Fig. 8A, B; Table 1). Binding affinity of the inhibitor NSC31867 for MtbNei2 was measured using SPR (Fig. 7C and Table 1). All three compounds were predicted to interact with the inter-domain catalytic-DNA binding cleft (Fig. 9A). NSC31867 forms H-bonds to the active site Pro2 and Ile62, Asn76 and Tyr166 (Fig. 9B i) and inhibits glycosylase activity. Moreover, the other two inhibitors NSC345647 and NSC250430 were predicted to form H-bonds with Ser61, Asn76, Arg77 and Tyr166. The latter residues are hypothesized to be involved in lesion recognition and void filling after base extrusion activities and inhibition of the glycosylase activity (Fig. 9B ii and iii).

4. Discussion

DNA repair mechanisms contribute to the survival and persistent infection of mycobacterium. *M. tuberculosis* genome is highly G/C rich which renders it to be more susceptible to oxidative DNA damage. This is the reason that *Mtb*'s DNA repair mechanism is highly evolved and it harbors at least three fpg/nei members and one Nth glycosylases as well as other BER factors to deal with this major problem. Occurrence of

multiple DNA glycosylases each specific for a particular type of base lesion enables pathogen to rectify a large spectrum of base lesions. The DNA Base excision repair is a premier pathway in *M. tuberculosis*, given the absence of a known mismatch repair pathway that is present in *E. coli*. Targeting this pathway can be a self-limiting strategy from the point of view of development of resistance as suggested earlier [23].

MtbNei2 (Rv3297) is a previously uncharacterized member of the DNA glycosylase family. MtbNei2 was found to bind undamaged and damaged DNA substrates. MtbNei2 specifically recognizes oxidized pyrimidines similar to its paralog MtbNei1. MtbNei2 removes base lesions not only on duplex DNA but also from single stranded, 5' fork, 3' fork and bubble DNA substrates like its prokaryotic and eukaryotic homologues. On the other hand, MtbNei2 possess Uracil DNA glycosylase activity unlike the *E.coli* homologue pointing to the significance of uracil repair in *Mtb*.

Another significant difference highlighted by the present study is that the Zn-finger motif in MtbNei2 is not essential for the glycosylase activity. Indeed the zinc-finger domain-deleted mutant MtbNei2ΔZNF was fairly active on the uracil containing DNA substrate (Fig. 6C). In our modeling experiments, despite having four cysteines in the extreme C-terminus, MtbNei2 exhibited an unstructured C-terminal zinc finger domain (Fig. 6Ai, iii). For instance, the human Nei1 contains a C-terminal zincless finger domain which interacts with many repair and replication factors [19–21]. Based on the activity of MtbNei2ΔZNF and modeling experiments, we hypothesize that the zinc-finger domain of MtbNei2 might similarly function as a protein-protein interaction domain.

Structural alignment of various members of fpg/nei superfamily indicated the conservation of active site residues (Pro2 and Glu3), helix two turn helix and zinc finger motif (4 cysteines). Complete loss of glycosylase activity observed in the active site mutants Nei2(P2A)-GST and Nei2(E3A)-GST of MtbNei2 strongly suggests that Pro2 and Glu3

are essential (Fig. 6).

The mutational analysis was helpful in selecting the target site on the protein for the virtual screening experiments against the NCI database. We identified three natural products, Norlobaric acid (NSC31867), Chaetochromin (NSC345647) and Gengetin (NSC250430) as inhibitors of both uracil DNA glycosylase activity as well as AP site cleavage activity of MtbNei2. Based on docking results, these inhibitors predictably interact with the active site of MtbNei2. The best of them, Norlobaric acid, binds to MtbNei2 with an affinity of 74 nM and has a relatively small core scaffold (Table 1). Residues (Pro2, Arg77 and Tyr166) involved in inhibitor binding as predicted by docking are well conserved in MtbNei1. Therefore, we hypothesize that the inhibitors identified in this study may inhibit MtbNei1 as well. These compounds represent the very first inhibitors against Nei and can form the basis of an inhibitor optimization program against mycobacterial BER.

Despite low sequence identity, both MtbNei1 and MtbNei2 have similar activities, conserved catalytic residues and DNA binding motifs (Fig. S5). Besides, both MtbNei1 and MtbNei2 could complement the spontaneous mutation frequencies of *E. coli* mutants [7]. These studies suggest that biological roles of MtbNei2 may be redundant with MtbNei1.

Acknowledgements

KL acknowledges Junior and Senior research fellowships from the Council of Scientific and Industrial Research, India. Dr. Sailesh Bajpai is acknowledged for discussion regarding SPR experiments. This work was supported by the Council of Scientific and Industrial Research through the SPLenDID grant [BSC0104]. This manuscript bears the CSIR-CDRI communication number 9537.

Appendix A. Transparency document

Supplementary data associated with this article can be found in the online version at <http://dx.doi.org/10.1016/j.bbrep.2017.07.010>.

Appendix B. Supplementary material

Supplementary data associated with this article can be found in the online version at <http://dx.doi.org/10.1016/j.bbrep.2017.07.010>.

References

- [1] V. Mizrahi, S.J. Andersen, DNA repair in *Mycobacterium tuberculosis*. What have we learnt from the genome sequence? *Mol. Microbiol.* 29 (1998) 1331–1339.
- [2] S.S. David, V.L. O'Shea, S. Kundu, Base-excision repair of oxidative DNA damage, *Nature* 447 (2007) 941–950.
- [3] M. Dizdaroglu, Base-excision repair of oxidative DNA damage by DNA glycosylases, *Mutat. Res.* 591 (2005) 45–59.
- [4] L. Aravind, D.R. Walker, E.V. Koonin, Conserved domains in DNA repair proteins and evolution of repair systems, *Nucleic Acids Res.* 27 (1999) 1223–1242.
- [5] J.A. Eisen, P.C. Hanawalt, A phylogenomic study of DNA repair genes, proteins, and processes, *Mutat. Res.* 435 (1999) 171–213.
- [6] S.S. Wallace, V. Bandaru, S.D. Kathe, J.P. Bond, The enigma of endonuclease VIII, *DNA Repair* 2 (2003) 441–453.
- [7] Y. Guo, V. Bandaru, P. Jaruga, X. Zhao, C.J. Burrows, S. Iwai, M. Dizdaroglu, J.P. Bond, S.S. Wallace, The oxidative DNA glycosylases of *Mycobacterium tuberculosis* exhibit different substrate preferences from their *Escherichia coli* counterparts, *DNA Repair* 9 (2010) 177–190.
- [8] D.O. Zharkov, G. Golan, R. Gilboa, A.S. Fernandes, S.E. Gerchman, J.H. Kycia, R.A. Rieger, A.P. Grollman, G. Shoham, Structural analysis of an *Escherichia coli* endonuclease VIII covalent reaction intermediate, *EMBO J.* 21 (2002) 789–800.
- [9] J.C. Fromme, G.L. Verdine, Structural insights into lesion recognition and repair by the bacterial 8-oxoguanine DNA glycosylase MutM, *Nat. Struct. Biol.* 9 (2002) 544–552.
- [10] A. Prakash, S. Double, S.S. Wallace, The Fpg/Nei family of DNA glycosylases: substrates, structures, and search for damage, *Prog. Mol. Biol. Transl. Sci.* 110 (2012) 71–91.
- [11] V.S. Sidorenko, M.A. Rot, M.L. Filipenko, G.A. Nevinsky, D.O. Zharkov, Novel DNA glycosylases from *Mycobacterium tuberculosis*, *Biochemistry* 73 (2008) 442–450.
- [12] N.K. Dutta, S. Mehra, P.J. Didier, C.J. Roy, L.A. Doyle, X. Alvarez, M. Ratterree, N.A. Be, G. Lamichhane, S.K. Jain, M.R. Lacey, A.A. Lackner, D. Kaushal, Genetic requirements for the survival of tubercle bacilli in primates, *J. Infect. Dis.* 201 (2010) 1743–1752.
- [13] H. Dou, C.A. Theriot, A. Das, M.L. Hegde, Y. Matsumoto, I. Boldogh, T.K. Hazra, K.K. Bhakat, S. Mitra, Interaction of the human DNA glycosylase NEIL1 with proliferating cell nuclear antigen. The potential for replication-associated repair of oxidized bases in mammalian genomes, *J. Biol. Chem.* 283 (2008) 3130–3140.
- [14] S.C. Lovell, I.W. Davis, W.B. Arendall 3rd, P.I. de Bakker, J.M. Word, M.G. Prisant, J.S. Richardson, D.C. Richardson, Structure validation by Calpha geometry: phi,psi and Cbeta deviation, *Proteins* 50 (2003) 437–450.
- [15] R. Mosca, T.R. Schneider, RAPIDO: a web server for the alignment of protein structures in the presence of conformational changes, *Nucleic Acids Res* 36 (2008) W42–W46.
- [16] E.F. Pettersen, T.D. Goddard, C.C. Huang, G.S. Couch, D.M. Greenblatt, E.C. Meng, T.E. Ferrin, UCSF Chimera—a visualization system for exploratory research and analysis, *J. Comput. Chem.* 25 (2004) 1605–1612.
- [17] G.M. Morris, R. Huey, W. Lindstrom, M.F. Sanner, R.K. Belew, D.S. Goodsell, A.J. Olson, AutoDock4 and AutoDockTools4: automated docking with selective receptor flexibility, *J. Comput. Chem.* 30 (2009) 2785–2791.
- [18] R. Karlsson, M. Kullman-Magnusson, M.D. Hamalainen, A. Remaeus, K. Andersson, P. Borg, E. Gyzander, J. Deinum, Biosensor analysis of drug-target interactions: direct and competitive binding assays for investigation of interactions between thrombin and thrombin inhibitors, *Anal. Biochem.* 278 (2000) 1–13.
- [19] T.R. O'Connor, R.J. Graves, G. de Murcia, B. Castaing, J. Laval, Fpg protein of *Escherichia coli* is a zinc finger protein whose cysteine residues have a structural and/or functional role, *J. Biol. Chem.* 268 (1993) 9063–9070.
- [20] S. Double, V. Bandaru, J.P. Bond, S.S. Wallace, The crystal structure of human endonuclease VIII-like 1 (NEIL1) reveals a zincless finger motif required for glycosylase activity, *Proc. Natl. Acad. Sci. USA* 101 (2004) 10284–10289.
- [21] P.M. Hegde, A. Dutta, S. Sengupta, J. Mitra, S. Adhikari, A.E. Tomkinson, G.M. Li, I. Boldogh, T.K. Hazra, S. Mitra, M.L. Hegde, The C-terminal domain (CTD) of human DNA glycosylase NEIL1 is required for forming BERosome repair complex with DNA replication proteins at the replicating genome: dominant negative function of the CTD, *J. Biol. Chem.* 290 (2015) 20919–20933.
- [22] TRIPOS, Inc., SYBYL Molecular Modeling Software Packages, Version X 2.0; TRIPOS, Inc.: St. Louis, MO, USA, 2012.
- [23] T. Khanam, R. Ravishankar, Exploiting bacterial DNA repair systems as drug targets: a review of the current scenario with focus on mycobacteria, *J. Ind. Inst. Sci.* 94 (2014) 1.